

Thermal Model for a High Temperature Active Magnetic Bearing

Luc Burdet¹, Beat Aeschlimann², Roland Siegwart¹

¹ Swiss Federal Institute of Technology (EPFL), Lausanne, Switzerland

² MECOS Traxler AG, Winterthur, Switzerland

luc.burdet@epfl.ch

Abstract

In order to design an AMB working at high temperature the thermal aspect has to be explored. The limitation of current must be determined as well as the temperature of work of the material. A steady state model including the thermal radiation has been built on the base of a thermal network. Temperature dependent thermal parameters of the component of the AMB were measured with experiments throughout a model fitting. This model programmed in MATLAB is fast enough to work in AMB optimization design routines. An application of choice of coil high temperature wires in function of their life span is presented.

Introduction

Active Magnetic Bearings (AMB) have the potential to be used in high temperature (HT) applications like micro gas turbines or jet engines. It is obvious, that the thermal and mechanical load of the materials in such applications is enormous. The materials have to be chosen properly and the magnetic bearings have to be well designed. It is essential to know the hot spot in the bearings in order to avoid damage of insulations and thus machine failures. On the other hand, there is few data about materials at high temperatures, which makes it difficult to find accurate models. In literature only a few reports on the topic can be found.

The Draper laboratory [1] did test on the soft magnetic material by exposing them at high temperature. The feasibility of AMB and gap sensor for application at high temperature has been already proven in [2] and [3]. None of the above-mentioned projects presented a detailed model suitable for designing high temperature magnetic bearings.

The present work focus thus on developing new design tools and materials for high temperature magnetic bearings.

This paper presents a thermal model, which allows the layout and optimization of HT bearings. It is based on a thermal network and is implemented in MATLAB. It has to be able to cope with temperature dependent parameters.

The thermal sources in an AMB are due to the losses of the electromagnetic system, which are the Joule losses in the actuator coils and the eddy current losses

in the magnetic material. They depend on the temperature and are non-linear effects. Furthermore, the bearing materials at high temperature have a significant "aging" with the time due to oxidation, diffusion or structural modifications.

The model enables to determine the thermal current limitation in the actuator coils, the current-force relation and other characteristics of the bearing. Furthermore it allows quantifying the life span of the AMB, which is limited by the "aging" of the material at high temperature.

This simplified, but powerful layout tool is used for the design of a HT bearing running at an ambient temperature of up to 500°C. The design is not the only goal of this model. It shall also be used to predict

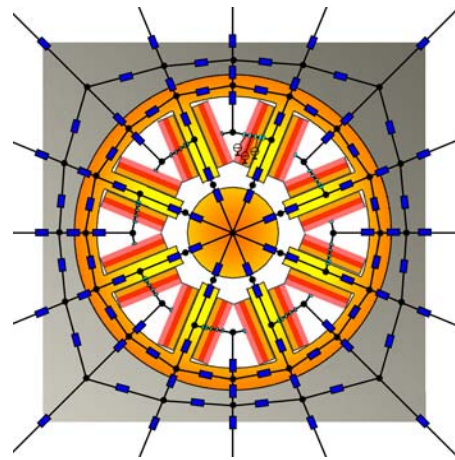


Figure 1: Thermal network of the AMB

deterioration of the AMBs. The algorithms shall be programmed effectively in order to keep computation time small. The results are verified in a HT AMB demonstrator rig.

Model Structure

The bearing model is realized as a thermal network. All elements are discrete, and transformed into heat resistances and heat sources (Figure 1). In this study, the problem is restrained to the static case, so the heat

capacitances in the network can be skipped (as explain in [6]) and the number of unknowns is minimized. The heat transfer can be described by three principles, where \dot{Q} [W] is the thermal power.

- *Conduction*: heat transfer in solid material

$$\dot{Q}_{cond} = \frac{\vartheta \cdot A}{L} \Delta T \quad (1)$$

Where ϑ [$\text{Wm}^{-1}\text{K}^{-1}$] is the thermal conductivity of the material, L [m] is the length between two points with temperatures T_1 and T_2 [K]. ΔT is the temperature difference $T_2 - T_1$. A [m^2] is the cross sectional area of the piece of material.

- *Convection*: heat transfer between solids and fluids

$$\dot{Q}_{conv} = \alpha \cdot S \cdot \Delta T \quad (2)$$

This coefficient α [$\text{Wm}^{-2}\text{K}^{-1}$] describes both the thermal conduction of the fluid and its motion. S [m^2] is the surface of the solid in contact with the fluid.

- *Radiation*: heat transfer through

For the case of the radiation some assumptions have been made. All the materials are considered as grey body. The coefficient of emission ε is considered equal to the coefficient of absorption. The radiation of the AMB to the environment is given by [5]

$$\dot{Q}_{rad} = \varepsilon \sigma (T_1^4 - T_a^4) S_1 \quad (3)$$

S_1 is the emitting surface and σ is the Stefan Boltzmann's constant, $\sigma = 5.67 \times 10^{-8} [\text{Wm}^{-2} \text{K}^{-4}]$. The thermal resistances of the network elements are given by:

- Conduction

$$G_{cond} = \frac{L}{\vartheta \cdot A} \quad (4)$$

- Convection

$$G_{conv} = \frac{1}{\alpha \cdot S} \quad (5)$$

- Radiation

$$G_{rad} = \frac{\Delta T}{\varepsilon \sigma (T_1^4 - T_a^4)} \quad (6)$$

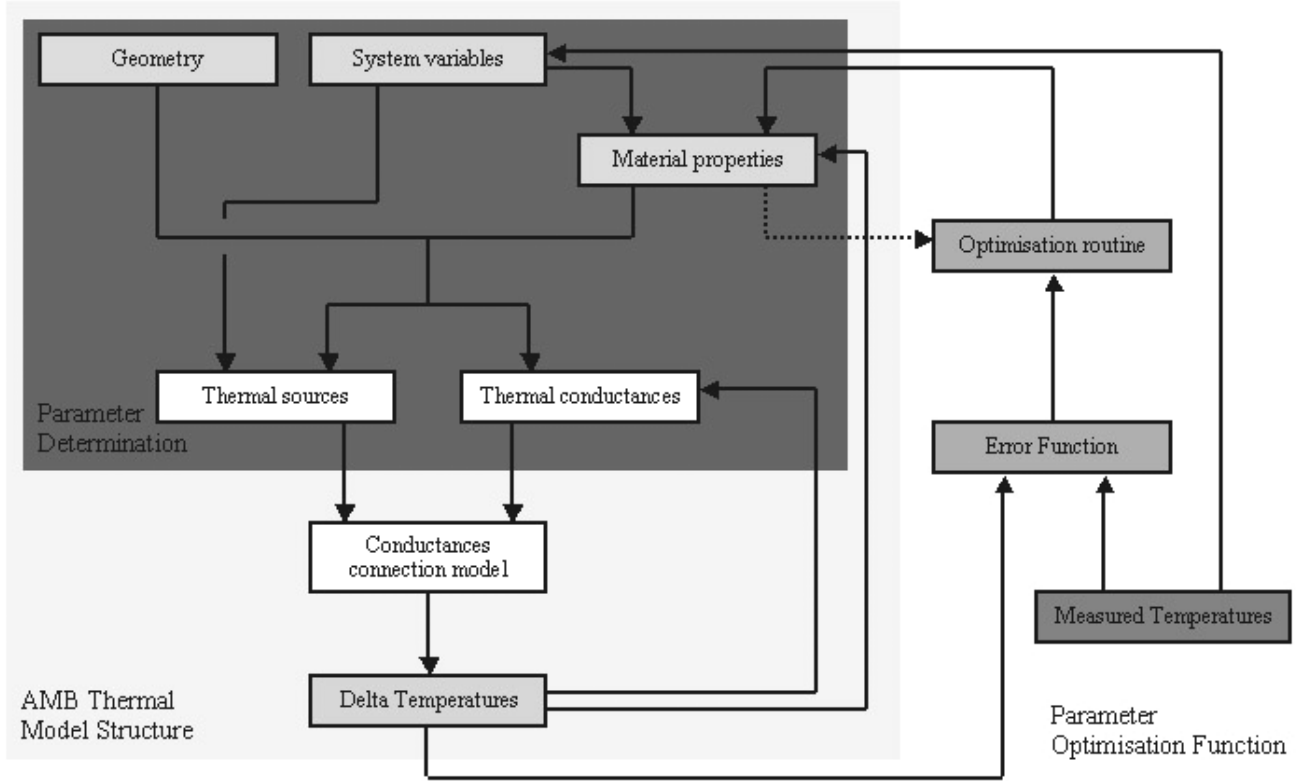


Figure 2: Block diagram of the thermal model

electromagnetic radiation

Some thermal parameters in equations (4)-(6) are temperature dependent. The nature of this dependency can be expressed by polynomials with unknown coefficients. These coefficients will be estimated during the model optimisation.

The electromagnetic system is discretized in a finite number of elements K_i . The states of the model are the temperatures T_i of each element. They are connected together by the thermal conductances G_{mn} of the matrix G (equation 7). This matrix G is square and symmetric. The temperatures T_i are obtained by inverting G .

$$\begin{pmatrix} G_{11} & G_{12} & \cdots & G_{1n} \\ G_{21} & G_{22} & \cdots & G_{2n} \\ \vdots & \vdots & \ddots & \vdots \\ G_{m1} & G_{m2} & \cdots & G_{mn} \end{pmatrix} \begin{pmatrix} T_1 \\ T_2 \\ \vdots \\ T_m \end{pmatrix} = \begin{pmatrix} \dot{Q}_1 \\ \dot{Q}_2 \\ \vdots \\ \dot{Q}_m \end{pmatrix} \quad (7)$$

Thermal Model

For simplicity, the model is built up in two modular steps, one for modeling only the coil (coil model) and one for the radial AMB including rotor, iron core, coils and housing (AMB model). As we can see in the block diagram of the figure 2, the model consists of three blocks. The first one reads a table containing the matrix G and reads the values from a file containing all the parameters of the AMB. Some of the parameters and conductances are dependent of the temperature and are directly connected to the calculated temperatures. The model proceeds also by iterations and try to converge to equilibrium. This optimisation loop represents the second block. The third block is a second optimisation loop, which compares the model predictions with measurements from the experimental rig and tunes the polynomial coefficients of the material properties accordingly.

Since the parameters and the thermal radiation depend on the temperature, a convergence problem is present. Introducing a factor, which reduces the influence of the calculated values on the initial temperatures for next iteration step, has solved this problem. The function “fmincon” of Matlab was used in order to do the parameter optimization. The medium-scale algorithm (line search) was used.

Coil Model

Coil wires with different insulations were used; a nickel-clad copper wire with an insulation of mica-fiberglass tape and an Inox-plated copper wire with a ceramic powder insulation between the conductor and the plating. The thermal resistance of the insulation is

very high compared to the one of copper. Furthermore the insulation layer is thick compared to the copper cross section.

In order to decrease the model complexity, a simple model of the coil has been chosen, which features:

- Static (steady-state) solution
- The temperature in the coil is constant in each layer of windings
- The radial thermal resistance of the copper is neglected compared to the radial thermal resistance of the insulation
- The axial conduction in the wire is simplified to the conductance of the copper, the conductance of the insulation is neglected

The coils were wound on ceramic coil holders, made of micanit. The relatively thick maintaining parts on the sides of the coil holders and the flat shape of the coils permit to restraint the number of thermal elements of one per layer by neglecting the side's effects.

AMB Model

The coil model is taken such as described in the last paragraph and it is inserted into a model containing the lamination of the stator, the housing block and the rotor. The heat transfer due to thermal conduction and the material parameters in function of the temperature are well known.

Without any rotation of the rotor and any forced airflow inside the furnace, the thermal convection is in this case only due to natural convection. In this case the Wong [4] and Hoffmann [5] give elaborated methods to model the natural convection. Examples with simple geometries of surfaces, like planes and tubes are usually given. In the case of AMB without rotor motion the airflow is due to the natural convection, also related to the acceleration of gravity, is different for each part of the stator. This phenomenon was approximated with a single parameter α for all the areas where convection takes place. An exception was made for the small air gap between stator teeth and rotor. Without motion of the rotor it is meaningful to consider a heat transfer mainly due to conduction of the air and not due to airflows. The parameter of the air conduction was used to model this case.

Based on the validated coil model, the whole AMB was modeled including thermal radiation and absorption. The values of the thermal radiation parameters are not given precisely in data sheets. They often depend on the temperature, the surface color of the material (may change due to oxidation) and on the experimentation.

The largest heat transfer due to the radiation is done at the hottest spots of the system, which are the coils in the case of AMB. The coils are divided in two parts, the coils head and the flat longitudinal parts. The coil heads radiate directly into the oven without reflection,

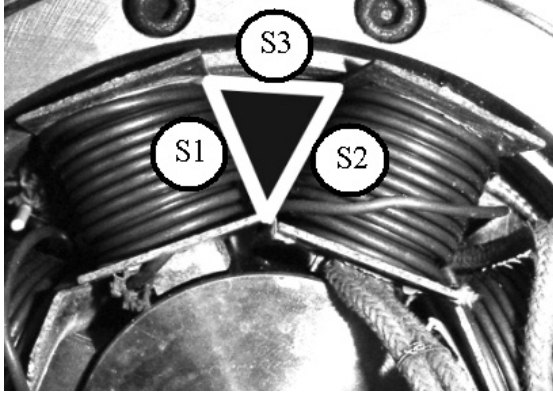


Figure 3: Area of thermal reflection

so equation (3) is used. In order to obtain a simple model, the longitudinal parts are considered as triangular spaces. The walls S_1 , S_2 (figure 3) are considered as the coils surface and S_3 the visible area of the stator. The illuminance J [Wm^{-2}] is a function of the emission flux ϕ_n and of the reflection flux of the three surfaces.

$$\begin{aligned} J_1 &= \phi_1 + (1 - \varepsilon_1)[F_{12}J_2 + F_{13}J_3] \\ J_2 &= \phi_2 + (1 - \varepsilon_2)[F_{21}J_1 + F_{23}J_3] \\ J_3 &= \phi_3 + (1 - \varepsilon_3)[F_{31}J_1 + F_{32}J_2] \end{aligned} \quad (8)$$

F_{mn} is the factor, which considers the angular orientation of surface S_m to surface S_n and ε_n their radiation coefficients. Equations (9) express the heat transfer from one surface to the others.

$$\begin{aligned} \dot{Q}_{12} &= F_{12}S_1(J_1 - J_2) \\ \dot{Q}_{13} &= F_{13}S_1(J_1 - J_3) \\ \dot{Q}_{1,23} &= S_1(J_1 - F_{12}J_2 - F_{13}J_3) = \dot{Q}_{12} + \dot{Q}_{13} \end{aligned} \quad (9)$$

By permutation of the indices the heat transfer of the other surfaces is obtained. In the present the areas S_1 , S_2 and S_3 are considered to be equal (assuming that the coil holder doesn't emit), so the factors F_{mn} are equal to 0.5.

Depending on the current feed symmetry of the setup is used to keep model complexity low. Computation time can be considerably reduced.

Experimental Results

At first several coils rolled on coil holders of ceramic were put in a furnace. The measured data were the applied voltage, the current inside the coil and the temperature inside the coil that was measured with an additional sensor. From these measurements the electric resistance of each wire in function of the temperature was extracted. After that DC current was applied to measure the coil temperature increase at different ambient temperatures.

In order to validate the AMB model an AMB test rig has been modified and equipped with resistance temperature sensors at different locations: Within the housing, inside a tooth, in the air between two coils, in the centre of the rotor and within a coil. They can measure up to 800°C . The coil temperature was also estimated by measuring its electrical resistance. The rotor has been fixed within the bearing enabling current variations without rotor motion. Rotor fastening parts have been designed as thin as possible to avoid heat transfer to the housing. Nevertheless, they have been included in the model.

The whole system was put in a furnace. A special care has been taken to thermally isolate the system as much as possible of the environment. The AMB housing was posed on very high and thin ceramic parts and not fixed with any metallic screws. Therefore there is no metallic contact of the housing with a base plate and thus no

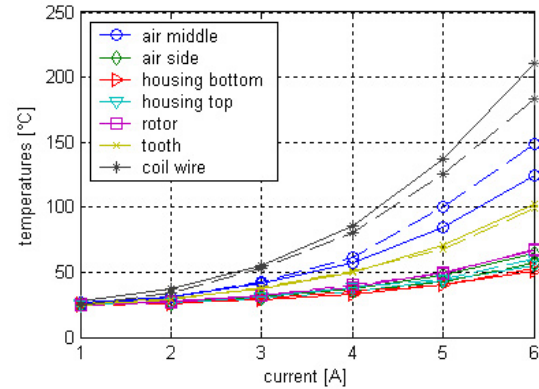


Figure 4: Comparison between the measured (dashed line) and the model temperature at 25°C ambient temperature

unmodeled heat losses. The furnace was heated up until reaching the steady state and then DC currents were applied in a pair of coils.

The data was acquired with a digital data acquisition system (Dspace) as well as a LCR meter related to Matlab during long-teem measurements.

The results are summarised in the figures 4, 5 and 6. For all these tests the same setup and the same model with the same parameters were used. The precision is only of 20% for the worst case in the figure 4, which is the temperature of the air between the coils at low temperature. The phenomenon for this case is only due to the convection of the air between the coils. A more analytical model should be done to obtain better results or to used forced airflow and have better known conditions. The temperature of the coil is also accurate only with 12.5 % between the prediction and the measure. We have to notice that the temperatures of the

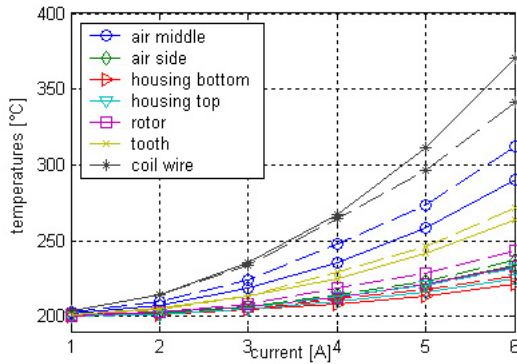


Figure 5: Comparison between the measured (dashed line) and the model temperature at 200°C ambient temperature

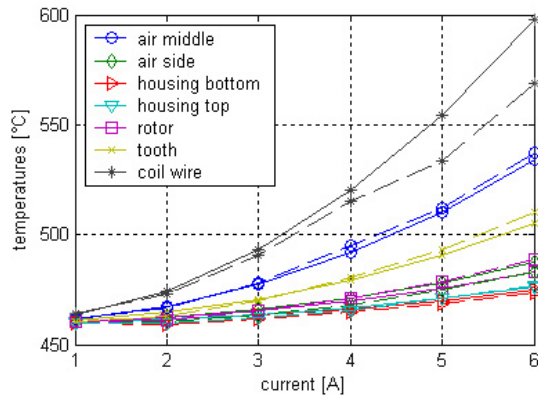


Figure 6: Comparison between the measured (dashed line) and the model temperature at 460°C ambient temperature

coils were estimated by measuring the electrical resistance of the coil. This estimation is also less accurate than a temperature sensor (1%) because of the low resistance of the coil (0.87 Ohm at 25°C), and also only small sensitivity ($\alpha_{Cu} = 0.004 \text{ K}^{-1}$) in function of the temperature. Otherwise the results are very satisfying and the values of the parameters are in the

ranges given in the literature [4]. The computation time is also very small, between 2.5 and 4 seconds depending of the current and environmental temperature.

Life Span Estimation

As said before, the aging of the material is a non-neglecting factor at high. For example in the case of nickel-clad copper wire, there is diffusion between the

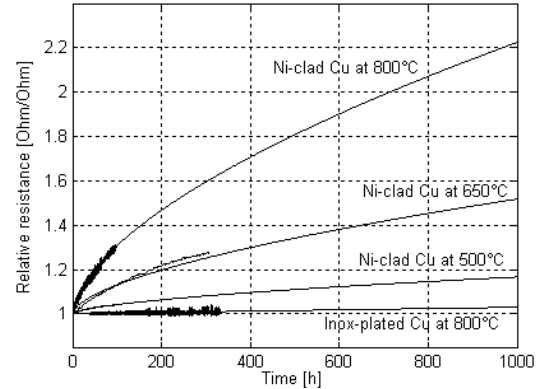


Figure 7: Increase of relative electrical resistance in function of the time

conductor and the cladding, which causes an increase of electrical resistance of the coils figure 5. Tests have been made at different temperatures for different materials during hundreds of hours and the curves have been approximated in order to predict the behavior of the materials after a very long time. The thermal model gives for example the temperature inside the coil layers in function of the current (Figure 8). So using the figures 7 and 8 we can find the life span in function of the current. As we can see in the figure 8 the number of layers are not the same for the different wires. In fact the same coil holder were used to compare the different

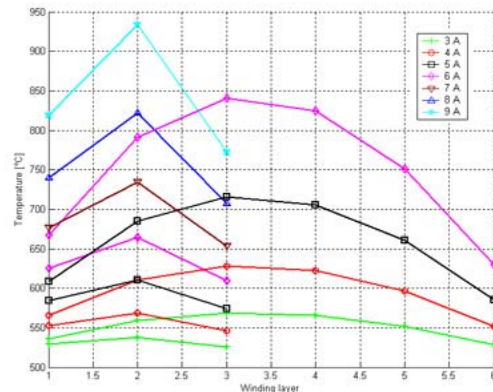


Figure 8: Comparison of the coil temperature in function of the current for Ni-clad Cu and Inox-plated Cu wires

technologies. So the number of turns for each coil is different, thus the available maximum force in function of the current is different. The fill factor for these two wires is also different, according to their insulation thickness, what gives the main difference in the available force. The figure 9 shows the two theoretical maximum forces (given in [7] and [8]) in function of the current for these technologies. As we can see, the saturation is for the Ni-clad Cu wire at about 4 [A]. With this current show a maximum wire temperature of 650°C what give already a limited very limited life span. Comparing to this, the Inox-plated Cu wire needs much more current to reach the saturation, because of a lower number of turns. Its temperature is also more than 950°C but its life span at this temperature is still long. A compromise has to be made between high efficiency and longer life span.

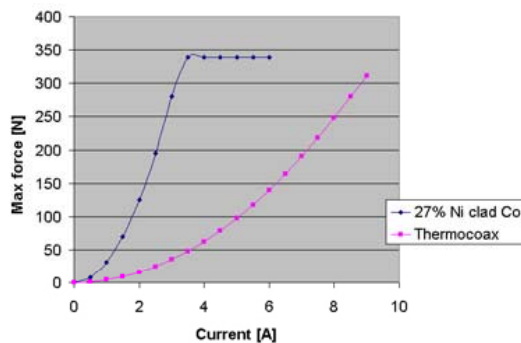


Figure 9: Maximum force of the AMB in function of the current

Conclusion

The presented thermal model permits to calculate the increase of temperature resulting from the thermal losses in a very wide range of temperature. The innovation is the inclusion of the thermal radiation effect in a relatively simple model. The fast and effectively programmed algorithms make it suitable for AMB design optimization.

Modeling first the coils to find their specific parameters and secondly find an optimized model of the whole system is the way to find the best technology, which gives the highest efficiency and life span.

Acknowledgment

This work is supported by the EC GROWTH Program, Research project “MagFly, Magnetic Bearings for Smart Aero Engines”, GRD1-2001-40 191.

References

[1] Kondoleon A.S., Kelleher W.P.: Soft Magnetic Alloys for High Temperature Radial Magnetic Bearings. *ISMB-7, Zürich, 2000*

[2] Mekhiche M., Nichols S., Oleksy J., Young J., Kiley J., Havenhill D.: 50 KRPM, 1,100°F Magnetic bearings for jet turbine. *ISMB-7, Zürich 2000.*

[3] Xu L., Wang L., Schweitzer G.: development of magnetic bearings for high temperature suspension. *ISMB-7, Zürich 2000.*

[4] Wong H. Y.: Heat transfer for engineers. *Longman Group Limited, London, 1977.*

[5] Hofmann H.: Phénomènes de transfert. *Laboratoire de Technologie des Poudres, EPFL / IMX.*

[6] Paychère C.: Conception d’entraînements électriques intégrés pour dispositifs multi-axiaux. *Thèse N° 1693, Ecole Polytechnique Fédérale de Lausanne, Lausanne, 1997.*

[7] Schweitzer G., Bleuler H., Traxler A.: Active magnetic bearings. *Hochschulverlag AG an der ETH Zurich, Zürich, 1994.*

[8] Siegwart R, Bleuler H, and Traxler A, Industrial Magnetic Bearings - Basics and Application, *Gordon and Breach Science Publisher, Amsterdam, 2000*